IOSR Journal of Computer Engineering (IOSR-JCE)
e-ISSN: 2278-0661, p-ISSN: 2278-8727, Volume 28, Issue 2, Ser. 1 (Mar. – Apr. 2026), PP 01-09
www.iosrjournals.org

Space Time Adaptive Processing Of Ground Surveillance Staggered PRF MTI Radar For Clutter Suppression

Venkata Krishna Rao Maddela
Independent Researcher, IEEE Senior Member
(Previously)Dept Of CSE (Data Science) & Dept Of Electronics & Communication Engineering,
Institute Of Aeronautical Engineering, Hyderabad, India

Abstract:
The conventional moving target indicator (MTI) radars perform doppler processing using MTI filters and FFT filter bank for ground clutter rejection and estimating the moving target parameters. The MTI radar suffers from clutter ridges at zero-doppler frequency. MTI filters are used to remove these clutter ridges, but MTI filters introduce the blind speeds. If phased array antennas are used to electronically scan the beam, Space Time Adaptive Processing (STAP) can be spatially filter out the clutter. In this work, a staggered pulse repetition frequency (PRF) MTI radar is simulated with long distant multiple targets and clutter with three PRFs. The conventional doppler filter bank and the STAP algorithm are implemented on radar return signals. The Range-Angle, the Doppler-Angle and the Velocity-Angle maps are produced in STAP analysis. The Range-Doppler map is generated for both conventional MTI and STAP receivers. Order statistic constant false alarm rate (OSCFAR) is applied on both the Range-Doppler maps to maximize the detection probability, and the target ranges and velocities are estimated. The measured ranges and dopplers are unwrapped to original values by least-squares grid search over a constrained solution space. Results show that the estimation errors are similar for both techniques, but the STAP successfully eliminated both the zero-frequency clutter and blind speeds without using any clutter cancellation filters.

Keywords - *Space Time Adaptive Processing, Staggered PRF, MTI Radar, Range-Doppler Map, Range-Angle Map, Doppler-Angle Map, MVDR beamformer*

Date of Submission: 27-02-2026 Date of Acceptance: 07-03-2026

I. Introduction

A pulse doppler or MTI radar illuminates the targets with RF radiation periodically at a rate of pulse repetition frequency (PRF) and estimates the two-way delay of echoes from targets to estimate its range and doppler shift to estimate the velocity. The range resolution is determined by the pulsewidth seconds and hence in practical radars the received echo signal is sampled at a sampling frequency of . The range is time-gated first and then at each time-gate the doppler frequency is estimated. For each PRF period , there are time-gates or range-gates or range-bins. The first range-gate is masked by the transmitted pulse, and hence the target echoes arriving after the first range-gate are processed to get the target range and doppler [1]. The unambiguous range of a pulse radar is given by

where c is the velocity of light in air, is the pulse repetition frequency of the radar. If the target range R is more than the unambiguous range , the target echo appears after the first PRF pulse, and hence the measured range wraps around and thus appears as . In general, if , the measured range is given by

where is the modulo operation. If the radar operates at three PRFs, the measured (wrapped) ranges are given by [2, 3]

At the receiver the wrapped ranges are to be unwrapped to a unique value . The effective unambiguous range of a staggered PRF radar is given by

where is the pulse repetition period of -th PRF and *P* is the number of PRFs. The effective range given by eq (4) is several orders higher than the unambiguous range obtained by any individual PRF. In practice such a huge range is practically not useful as the radar transmitter needs huge powers to illuminate the targets at that range. Hence the number of PRFs are mostly limited to 3 or 4 in practice.

The unambiguous doppler frequency of the pulse radar is given by

The doppler frequency of a target travelling with velocity is given by

Here sign represents a target approaching the radar and sign represents a receding target. If the target doppler is more than the unambiguous doppler , the measured doppler appears as . In general, if the , the measured doppler appears as . Mathematically the wrapped measured doppler frequency (one per each PRF) is given by [3, 4]

At the receiver the three wrapped dopplers are to be unwrapped to a unique value and then the velocity is estimated from the estimated doppler as

If multiple PRFs are selected to have small non-integer ratios, then the radar is called a staggered PRF radar. The staggered PRFs will eliminate the blind speeds associated with MTI radar with single PRF and drastically extends radar's unambiguous doppler frequency which is given by

The effective unambiguous range of a staggered PRF radar can be shown to be [3]

The effective doppler given by eq (10) is several orders higher than the unambiguous doppler obtained by any individual PRF. In practice such a huge doppler is practically not useful as the radar receiver must have such a huge bandwidth and the huge doppler may not be produced in the field. Hence the number of PRFs are mostly limited to 3 or 4 in practice.

The traditional moving target indicator (MTI) radars perform range-doppler processing using MTI filters or doppler filter bank [3, 4] to detect moving targets by rejecting ground clutter. The radar doppler processing is an age-old problem and lots of literature discussed related problems [5, 6, 7, 8, 9]. C. Cao, et. al [10] proposed a low-rank representation to separate the target from clutter. With the maturity of direction-of-arrival techniques, spatial time processing emerged as a promising technique to eliminate or mitigate the ill-effects of blind speeds. Parisa, P. al [11] implemented a range-gated Doppler filterbank on a 16-bit Texas processor. The paper also reported the simulation studies on a hybrid of a P-order autoregressive model and N-point FFT technique for suppressing ground clutter. Mohammad A. R., et. al. [12] provided yet another review of fundamentals of staggered MTI radar. Riabukha, V.P., et. al [13] performed experiments on an MTI system based on adaptive lattice filter and showed that the adaptive filters outperformed the traditional MTI system. The phased array antennas with the capability of electronically scanning the beam made the spatial time processing easy and popular [14, 15]. The phased arrays have been successfully used for spatially filtering for dynamically suppressing interference by creating nulls in the radiation pattern. Such processing is known as spatial time adaptive processing (STAP). Modern radar and communication receivers are designed to have STAP capability. Good amount of research has been reported and continues to be an active research area [16, 17, 18]. Jingwei Xu, et.al [19] proposed a frequency diverse array for MIMO STAP radar that uses space-time-range adaptive processing (STRAP) to suppress interference and jammers. It works based on a subspace projection technique and provides degrees of freedom in both range and angles.

In the present study the echo signals of a staggered pulse repetition frequency (SPRF) MTI radar engaged in multi-target and environment are simulated using the radar and target parameters. The conventional MTI doppler filterbank and the STAP algorithm are implemented on radar return signals. The Range-Doppler map is generated for both convention MTI and STAP receivers. The Range-Doppler maps are processed by order statistic constant false alarm rate (OSCFAR) detection technique, and the target ranges and velocities are estimated. The measured ranges and dopplers are unwrapped to original values by least-squares grid search. It is shown that though the estimation errors are similar for both techniques, the STAP successfully eliminated both the zero-frequency clutter and blind speeds without using any clutter- cancellation filters. The term "STAP" is used in this study, because data adaptive sample matrix inversion (SMI) beamforming is used to suppress the clutter.

After introducing the fundamental theory of MTI pulse doppler radar in section I, the rest of the paper is organized as follows. In section II the methodology for the implementation of conventional MTI and STAP analysis is discussed. In Section III the details of simulations and simulations environment and the results are discussed. In Section V conclusions are drawn and scope of future work is projected.

II. Methodology

In ground surveillance STP radar the antenna beam is scanned step-by-step in azimuth. At each beam position the returns from targets or clutter lying within the beam are received at the input of phased array antenna of the radar receiver. These signals are scaled by complex weights and summed that appear at the RF input of the radar. The signal received is range-gated and doppler analyzed for each beam position. Thus, there is one Range-Doppler (RD) map for each azimuth angle. If there are range bins and doppler filters, then size of the RD map is For each range bin there is one Doppler-Angle (DA) map which depicts the targets of moving with different velocities over an azimuth angle range. If there are angle positions, then size of the DA map is Similarly for each doppler bin there is one Range-Angle (RA) map of size is gives the distribution of targets or clutter at different ranges over an azimuth angle range.

The steering angle is the physical direction of the beam relative to the array broadside (here). In space–time processing steering angle is called the spatial frequency. The array element weights are considered as signal samples in space, with a spacing of interelement distance. When a constant real amplitude (unity) input signal is applied at the array input, the antenna outputs become these weights. Since the beam radiation pattern is the fourier transform of these samples, the quantity given below

is called a spatial frequency which corresponds to an angle in space. The quantity is also called a steering angle, as it determines the angle of beam. Accordingly, the spatial steering vector corresponding to beam angle is given by

where is the number of array elements. To perform doppler analysis the echo signal is sampled at PRI interval . This is equivalent to a sampling frequency of . When discrete fourier transform is performed on these samples, we get the complex frequency spectrum with the frequency range, . Each frequency in the range corresponds to a target velocity . Accordingly, the temporal steering vector corresponding to doppler is given by

The steering vectors given by eq (11) and eq (12) are separable and can be combined to form a single vector called spatiotemporal steering vector. The set of all spatiotemporal steering vectors can be expressed as the knocker product of and

This matrix is of size .

III. Traditional MTI Range–Doppler processing:

For a given range bin and for number of PRF echo pulses received, the -th Doppler filter output is computed as

where are signal sampled at a sampling period of ; these are called slow-time samples against the range-gate samples at a sampling period of , which is very small compared to . Accordingly, the range-gate samples are called fast-time samples. The eq (15) is the discrete fourier transform (DFT) of the signal Considering all range bins, we have a matrix

for . Then the Range-Doppler map is defined by

IV. STAP Based MTI Range–Doppler Processing:

The space-time snapshot of received signal for a given range bin is formed by stacking space-time samples into a matrix, called STAP snapshot and is given by

where is the number of array elements and is the number slow-time samples or snapshots, and is the frame number, each frame having snapshots. The number of frames for collecting data requirements of the beamforming algorithm or limited by the radar system parameters. Each column in is a snapshot of receiving antenna array inputs at some instant. Thus, the last column = **x(n)** is the snapshot at -th discrete instant and the first column is the snapshot at **-**th discrete instant i.e., instants prior to -th instant. The covariance matrix of -th frame of the received signal is given by

This matrix is called *sample covariance matrix*. If the signal is collected for frames, then we get an aggregate covariance matrix as

By applying diagonal loading to the matrix we get

Where is the noise power which can be estimated from the snapshots where there is no desired (target) signal. Alternatively, a small quantity (is normally used. The inverse of this covariance matrix is used to arrive at the STAP adaptive filter weights to form the beam. The weights are given by [20]

where the weight vector **(**k**)** is of size and is applied on the -th spatiotemporal steering vector to form the beamformer output

where denotes Hermitian transpose. For each doppler frequency, , we have one steering vector of size .. Number of discrete dopplers used is same as the number of snapshots. Then for each range bin we have an output vector is of size . Thus we can build a STAP Range–Doppler map as

The eq (14) is popularly known as *capon* or *minimum variance distortionless response* (MVDR) beamformer. It is based on the sample matrix inversion (SMI) [20]p

Algorithm for traditional MTI processing:

1. Initiate the Range-Doppler map with all zeros; being the number of PRFs.
2. Initiate the PRF loop.
3. Read the radar echo data of first PRF from to data matrix
4. Read the data snapshot of first range bin from to
5. Compute the row wise fast fourier transform (FFT) of and store in .
6. Compute the squared absolute value .
7. Compute column wise sum store the sum as a row in .
8. Go to next row: .
9. Check for . If No go to step 4, else go to next step.
10. Check for . If No go to step 3, else go to next step.
11. Stop.

Algorithm for STAP MTI processing:

1. Initiate the Range-Doppler map with all zeros; being the number of PRFs.
2. Create the doppler bins in the range: with equal spacing i.e.,
3. Initiate the PRF loop.
4. Read the radar echo data of -th PRF from to data matrix
5. Set range bin ; being the number of training bins on either side of range bin (say 4 here).
6. Read the signal snapshot of current range bin into
7. Read the signal snapshots of the range bins: excluding the current range bin from data matrix to where . A total of signal snapshots around the current range bin are read.
8. Set ; Initialize the sample covariance matrix with zeroes.
9. Read the signal snapshot into .
10. Column-by-column flatten the to a vector of size: .
11. Compute the outer product and accumulate as
12. Set . Check for , if No go to step 9, else go to next step.
13. Compute ; Diagonally load .
14. Compute the inverse .
15. Compute the spatiotemporal steering vectors: for broadside angle: for doppler frequencies in the range: using eq (13).
16. Compute the STAP weights, for all
17. Read the signal snapshot of the range bin: and flatten.
18. Compute the STAP output,
19. Compute the squared absolute value , store in .
20. Go to next range bin. .
21. Check for . If No go to step 6, else go to next step.
22. Go to next PRF: . Check for . If No go to step 4, else go to next step.
23. Stop.

Post Processing:

Step1: CFAR based Target Detection:

The Range-Doppler map is processed by the OS-CFAR based Target Detection algorithm [1,3] to increase the detection probability. A

Step2: Joint Range-Doppler Disambiguation [3]

The range estimate and doppler estimate are jointly least-squares searched over the range space: such that the following condition

and over the doppler space: such that the following condition

is satisfied on a 2-D grid. The optimum solution is the range and doppler estimates.

V. Simulations And Results

1. Data Generation:

The required radar returns of the staggered PRF MTI radar are simulated using the algorithm discussed in another study [21] by the author. The latter two PRFs form ratios with the first PRF are 0.9130 and 1.0870 respectively. It may be verified that these PRFs combinedly offer an unambiguous range of 10000 km, as computed by eq (4) and an unambiguous doppler of 7.4 MHz (approx.) as computed by eq (10). Data is simulated using the radar and array parameters given in Table 1 with the number of array elements , and the target parameters given in Tables 2 to 4. The data is stored in a *Datacube* structure one for each PRF [21].

Table1. Radar System Parameters

	PRF: 13.695 kHz		PRF: 15 kHz		PRF: 16.305kHz	
Pulse Repetition Interval (s)	73.02		66.67		61.33	
Operating Frequency (GHz)	10		10		10	
Operating Wavelength (m)	0.30		0.30		0.30	
Pulse width s)	1		1		1	
Range Resolution (m)	150		150		150	
No. of Range bins, Nr	73		66		61	
Unambiguous Range Limits (m)	15	10950	15	9990	9195	
Unambiguous Doppler Limits (Hz)	-6847.5	6847.5	-7500	7500	-8152.5	8152.5
Unambiguous Velocity Limits (m/s)	-102.7	102.7	-112.5	112.5	-122.3	122.3
No. of Doppler bins/Pulses, N	64		64		64	
Doppler Resolution (Hz)	213.98		234.38		254.8	

The traditional MTI and STAP techniques are implemented using algorithms given in section III. The Range-Angle Maps at SNR of 10dB for three PRFs are shown in Figures 1 to 3. The Range-Angle (RA) map, The Doppler-Angle (DA) map and the Velocity-Angle (VA) map discussed in [3, 21] for three PRFs are shown in Figures 1, 2 and 3 respectively. The target and clutter amplitudes are respectively determined by the target power-to-noise ratio (SNR) of 10dB and clutter power-to- noise ratio (CNR) of 10dB. The targets appear as points in RA map, as they are point sources. However, in DA and VA maps they appear blurred along azimuth angle due to the scanning of antenna array beam of finite width. During scanning the antenna beam convolves with the point target reflectivity. There is no blurring along range direction as there is no scanning in the radial direction. While scanning the beam moves away from the broadside zero angle, the beam broadens and hence at higher angles the targets are more blurred.

Table 2. Target Range Details (used for simulations)

Parameter (units)	PRF-1 13.695 kHz	PRF-2 15 kHz	PRF-3 16.305kHz
Max Unambiguous Range (m) of Radar	10953	10000	9200
Max Unambiguous Range bin	73	67	61
Target-1			
True Range (m)	7500	7500	7500
Folded/Ambiguous Range (m)	7500	7500	7500
Number of Folds (f)	0	0	0
Range bins of True Range	50	60	60
Range bins of Ambiguous Range	50	50	50
Target-2			
True Range (m)	14500	14500	14500
Folded/Ambiguous Range (m)	3547	4500	5300
Number of Folds	1	1	1
Range bins of True Range	97	97	97
Range bins of Ambiguous Range	24	30	36
Target-3			
True Range (m)	19000	19000	19000
Folded/Ambiguous Range (m)	8047	9000	600
Number of Folds (f)	1	1	2
Range bins of True Range	127	127	127
Range bins of Ambiguous Range	54	60	5
Target-4			

True Range (m)	25000	25000	25000
Folded/Ambiguous Range (m)	3094	5000	6600
Number of Folds (f)	2	2	2
Range bins of True Range	167	180	180
Range bins of Ambiguous Range	21	33	45

Table 3. Target Doppler Details (used for simulations)

Parameter (units)	PRF-1 13.695 kHz	PRF-2 15 kHz	PRF-3 16.305kHz
Max Unambiguous Doppler (Hz) of Radar	6848	7500	8153
Max Unambiguous Doppler bin	64	64	64
Target-1			
True Doppler (Hz)	12000	12000	12000
Folded/Ambiguous Doppler (Hz)	5153	4500	3848
Number of Folds (f)	1	1	1
Doppler bins of True Doppler	112	102	94
Doppler bins of Ambiguous Doppler	48	8	
Target-2			
True Doppler (Hz)	14667	14667	14667
Folded/Ambiguous Doppler (Hz)	972	7169	6514
Number of Folds	2	1	1
Doppler bins of True Doppler	138	126	116
Doppler bins of Ambiguous Doppler	10	62	52
Target-3			
True Doppler (Hz)	24667	24667	24667
Folded/Ambiguous Doppler (Hz)	4124	2167	209
Number of Folds (f)	3	3	3
Doppler bins of True Doppler	231	211	194
Doppler bins of Ambiguous Doppler	39	19	2
Target-4			
True Doppler (Hz)	20667	20667	20667
Folded/Ambiguous Doppler (Hz)			
Number of Folds (f)	3	2	2
Doppler bins of True Doppler			
Doppler bins of Ambiguous Doppler			

Table 4. Target Velocity Details (used for simulations)

Parameter (units)	PRF-1 13.695 kHz	PRF-2 15 kHz	PRF-3 16.305kHz
Max Unambiguous Velocity (Hz) of Radar	1027	1125	1223
Max Unambiguous Velocity bin	64	64	64
Target-1			
True Velocity (m/s)	-1800	-1800	-1800
Folded/Ambiguous Velocity (Hz)	-773	-675	-577
Target-2			
True Velocity (m/s)	2200	2200	2200
Folded/Ambiguous Velocity (m/s)	146	1075	977
Target-3			
True Velocity (m/s)	3700	3700	3700
Folded/Ambiguous Velocity (m/s)	619	325	31
Target-4			
True Velocity (m/s)	-3100	-3100	-3100
Folded/Ambiguous Velocity (m/s)	-19	-850	-654

It may be noted that the Range-Velocity maps of traditional MTI processing in Figures 4(a), 5(a) and 6(a) are relatively smoother compared to their counterparts of STAP analysis. It is because the doppler FFT works as a bank of narrowband filters, and each filter eliminates the out-of-band noise thus significantly improving the output SNR. The improvement in SNR depends on the number of FFT bins (64 filters for positive doppler axis and 64 filters for negative doppler axis), we get an SNR improvement of is independent of PRF. The vertical strip at zero velocity is created due to the stationary clutter (velocity = doppler = 0). This strip is called clutter ridge. However, in Figures 4(b), 5(b) and 6(b) no such ridge exists which is the biggest advantage of STAP. The Range-Velocity maps of STAP analysis are noisy because only one frame of snapshots is used i.e., in eq (17) – eq (19). The spreading of target horizontally along doppler axis also occurred in case of MTI. It is due to the sidelobes of individual doppler filterbank responses. Since no window function is used explicitly, the default window is rectangular whose spectrum has a highest sidelobe level of -13.5dB. As there is no FFT involved in STAP, no such target blurring is observed in STAP.

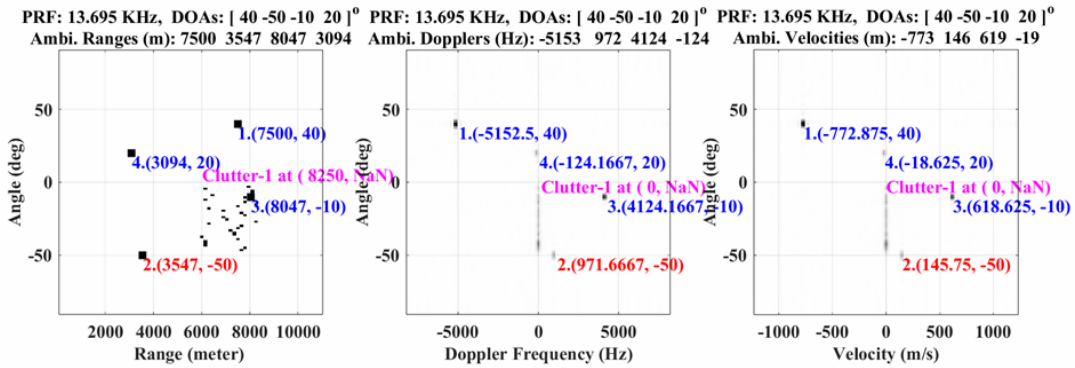

Figure 1. STAP analysis (a). Doppler-Angle Map (b). Velocity-Angle Map for first PRF.

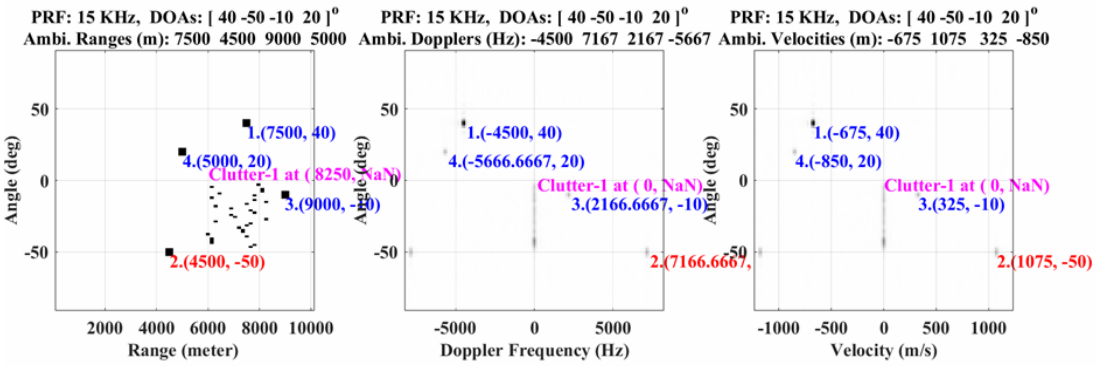

Figure 2. STAP analysis (a). Doppler-Angle Map (b). Velocity-Angle Map for second PRF.

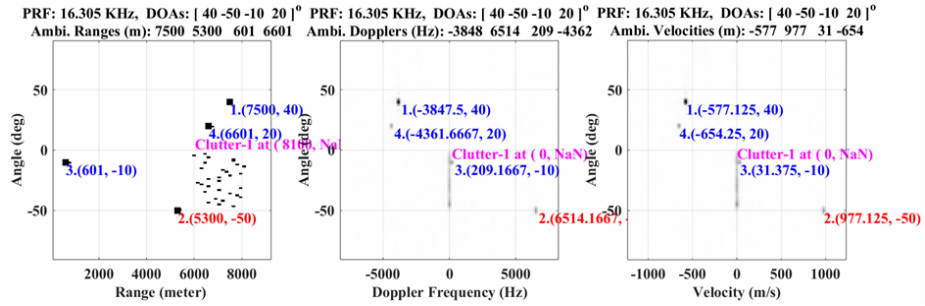

Figure 3. STAP analysis (a). Doppler-Angle Map (b). Velocity-Angle Map for third PRF.

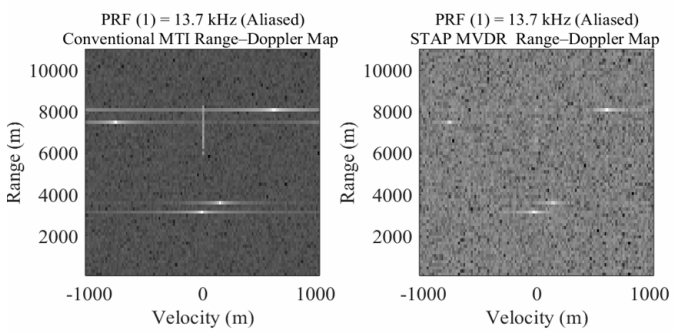

Figure 4. Velocity- Range Map for PRF-1 (a). Traditional MTI (b) STAP MTI ()

To estimate the target parameters frames are averaged to estimate the covariance matrix for STAP analysis. Eight train cells, two guard cells, and OS rank of 0.75 are used for CFAR analysis. The detection threshold is adjusted to get the best results. A search space of is used for disambiguation of range. A search space of corresponding to is used for velocity disambiguation.

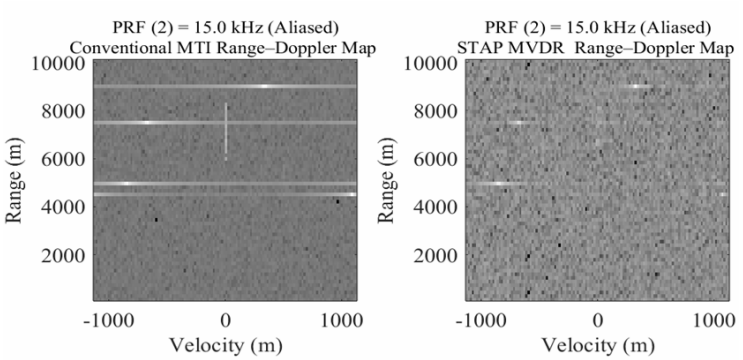

Figure 5. Velocity- Range Map for PRF-2 (a). Traditional MTI (b) STAP MTI ()

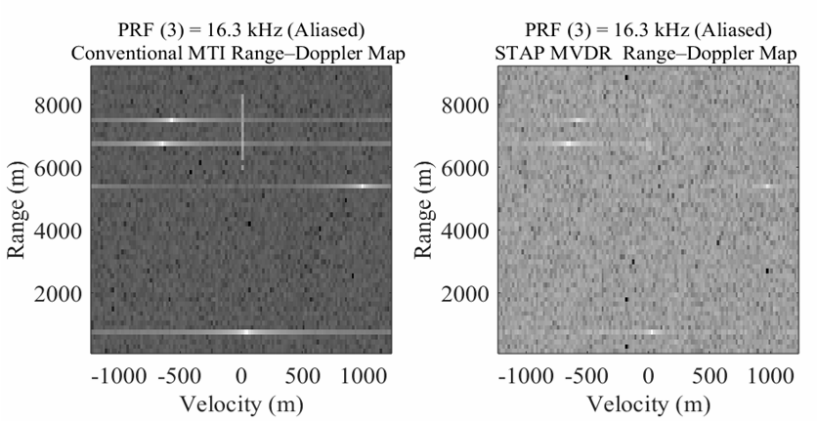

Figure 6. Range-Velocity Map for PRF-3 (a). Traditional MTI (b) STAP MTI ()

Table 5. Performance of Traditional MTI and STAP MTI radar

	Traditional MTI			STAP MTI		
Parameter (units)	True	Estimate	%Error	True	Estimate	% Error
Target-1 Range (m)	7000	7450	-6.00	9000	8550	5.00
Target-2 Range (m)	14500	13900	4.13	14500	14950	3.10
Target-3 Range (m)	19000	19300	-1.59	19000	19300	1.50
Target-4 Range (m)	27000	27450	-1.80	27000	24550	-2.80
Target-1 Velocity (m/s)	-1800	-1736	3.56	-1800	-1736	3.56
Target-2 Velocity (m/s)	2200	2120	3.64	2200	2136	2.91
Target-3 Velocity (m/s)	3700	3828	-3.46	3700	3796	-2.59
Target-4 Velocity (m/s)	-3100	-3212	-3.61	-3100	-3180	-2.58

VI. Conclusions And Future Work

The conventional MTI doppler filterbank and the STAP algorithm are implemented on the simulated radar return signals. The Range-Doppler map is generated for both convention MTI and STAP receivers. The Range-Doppler maps are used to detect the moving targets using CFAR (Order Statistics) and estimate the target ranges and velocities. The measured ranges and dopplers are unwrapped to original values by least-squares grid search using Chinese remainder theorem (CRT). It is shown that the estimation errors are almost same for both techniques. But the STAP successfully eliminated both the zero-frequency clutter and blind speeds without using any MTI cancellation filters. The Range-Velocity maps of STAP analysis are noisy since only one frame (less data) is used in this study. By using more frames for covariance matrix computation, STAP Range-Velocity map can be made cleaner. Despite the advantages of STAP compared to MTI as discussed in results section, it has certain disadvantages (1). Needs more training data to get better estimate of covariance matrix. (2). Higher computation complexity but it won't miss the targets as is the case with MTI. In general, the PRFs used for Ground Surveillance radar are lower compared to the PRFs used in this study. The higher PRFs are used in this study to reduce the number of maximum range bins and simulation time. However the methodology and results of this study are generic and applicable for any radar parameters.

The limitations of this work include the use of point targets, stationary clutter, AWG noise, no jammers and only azimuth plane. Future work can be continued to include targets that extend over multiple range bins, moving clutter and adaptive suppression of jammers, non-homogeneous clutter, non-gaussian and correlated noise, range bin migration and elevation angle i.e., 3D STAP processing.

References

[1] Merrill I. Skolnik, Introduction To Radar Systems, 2nd Edition, 1981, Mcgraw-Hill.
[2] Trunk, Gerard V. And Steven M. Brockett. "Range And Velocity Ambiguity Resolution." The Record Of The 1993 IEEE National Radar Conference (1993): 146-149
[3] Richards M.A. *Fundamentals Of Radar Signal Processing* Mcgraw-Hill New York 2014
[4] Fred E Nathanson, Radar Design Principles, 2nd Edition, 1991, Mcgraw-Hill.
[5] V. C. (Chris) Sullivan, Radar Foundations For Imaging And Advanced Concepts, Scitech Publishing, IET, 2019.
[6] Schleher, D. C., Performance Comparison Of MTI And Coherent Doppler Processors, Radar 82,IEE Conf Pubno 216, Oct 82: 154-158.
[7] E. D'Addio, A. Farina & F. Studer, Performance Comparison Of Optimum And Conventional MTI And Doppler Processors, IEEE Trans. Aerospace And Electronic Systems, 1984: 707-715
[8] Marzetta, T. L., A New Method For Coherent Integration While Explicitly Accounting For Range Bin Migration, IEEE Transactions On Aerospace And Electronic Systems, Vol. 29 (4), 1993: 1388-1393.
[9] S. Bidon, L. Savy And F. Deudon, Fast Coherent Integration For Migrating Targets With Velocity Ambiguity, IEEE Radarcon (RADAR), Kansas City, 2011: 27-32.
[10] C. Cao, Et. Al., Clutter Suppression And Target Tracking By The Low-Rank Representation For Airborne Maritime Surveillance Radar," *IEEE Access*, 2020, 8: 160774-160789. Https://Doi.Org/10.1109/ACCESS.2020.3021124
[11] Parhizgar, Parisa Et. Al. Implementation Of Digital Signal Processor For Pulse Doppler Radar. Computer Networks And Communications. 2023; 1(2): 309-324 Https://Doi.Org/10.37256/Cnc.12202336 89
[12] Mohammad A. Rahaman, Et. Al., A Study On Digital MTI Processors & Frequency Pulse, International Journal Of Innovative Science And Research Technology, October 2025, 10(10): 1820-1837. Https://Www.Ijisrt.Com/A-Study-On-Digital-Mti-Processors-Frequency-Pulse
[13] Riabukha, V.P., Semeniaka, A.V.,. Et Al. Comparative Experimental Investigations Of Adaptive And Non-Adaptive MTI Systems In Pulse Radars Of Various Applications And Wave Ranges. *Radioelectronics And Communications Systems,* 2022, 65:165–176. Https://Doi.Org/10.3103/S073527272204001X
[14] B. D. Van Veen And K. M. Buckley, "Beamforming: A Versatile Approach To Spatial Filtering," *IEEE ASSP Magazine*, April 1988, 5(2): 4-24, Https://Doi.Org/10.1109/53.665
[15] R. C. Hansen, Phased Array Antennas, 2nd Edition, 2009, John Wiley & Sons, Inc.
[16] Robert J. Mailloux, Phased Array Antenna Handbook, 2nd Edition, Artech House, Inc., 2005, Norwood, MA.
[17] Robert A. Monzingo, Randy L. Haupt And Thomas W. Miller, Introduction To Adaptive Arrays, 2nd Edition, 2011, Scitech, Raleigh.
[18] Sergiy A. Vorobyov, Principles Of Minimum Variance Robust Adaptive Beamforming Design, Signal Processing, Vol. 93 (12), 2013: 3264-3277 Https://Doi.Org/10.1016/J.Sigpro.2012.10.021
[19] Jingwei Xu, Shengqi Zhu, And Guisheng Liao, Space-Time-Range Adaptive Processing For Airborne Radar Systems, IEEE Sensors Journal, March 2015, 15(3):1602-1610. Https://Doi.Org/10.1109/JSEN.2014.2364594
[20] Guerci, J. R. *Space-Time Adaptive Processing For Radar*. Artech House Radar Library. Boston: Artech House, 2003.
[21] Krishna Rao M.V., A Staggered PRF MTI Ground Radar Simulator For Space Time Processing In Multi-Target And Jamming Environments, IOSR Journal Of VLSI And Signal Processing (IOSR-JVSP)**,** Vol. 16 (2), Jan-Feb 2026, pp. xx-xx (Accepted For Publication).